Desalination and Water Treatment
www.deswater.com

doi: 10.5004/dwt.2022.28410

256 (2022) 176–193
April

The effect of activated carbon produced from remnants of walnut shell and ox tongue leftover on removing cadmium metal from water

Esmail Mohseni[a], Elham Rostami[b], Zahra Hamdi[a], Morteza Mortezavi Mehrizi[c], Abdolrasoul Rahmani[d,*]

[a]*Department of Environmental Health Engineering, School of Health, Larestan University of Medical Sciences, Larestan, Iran, emails: mohseniesmail210@gmail.com (E. Mohseni), Zhamdi2015@yahoo.com (Z. Hamdi)*
[b]*Department of Chemistry, Faculty of Science, Shahid Chamran University of Ahvaz, Ahvaz, Iran, email: Elhamrostami74@gmail.com*
[c]*Department of Occupational Health Engineering, School of Public Health, Shahid Sadoughi University of Medical Sciences, Yazd, Iran, email: Matinmehrsa1360@gmail.com*
[d]*Department of Occupational Health and Safety, School of Health, Larestan University of Medical Sciences, Larestan, Iran, Tel. +98 9104553160; Fax: +98 24 3305 2477; email: rahmaniabdolrasoul218@gmail.com*

Received 5 September 2021; Accepted 17 March 2022

ABSTRACT

Heavy metals are dangerous pollutants in surface water and groundwater resources causing health risks for human and environment. In this study, activated carbons extracted from walnut shell (ACWS) and ox tongue leftover (ACO), as two low-cost and green sorbents, were synthesized via chemical activation with different concentrations of phosphoric acid (20%–80% w/w) at two temperatures (500°C and 700°C) for removal of cadmium ions from aqueous solutions. To compare ACWS and ACO, Fourier-transform infrared spectroscopy, X-ray powder diffraction analysis, field-emission scanning electron microscopy, and energy-dispersive X-ray spectroscopy were performed. The effect of initial concentration of cadmium, contact time, pH, and amount of adsorbent on the adsorption process was studied through a batch process mode. Both ACWS and ACO successfully removed cadmium metal with about 90.66% and 89.33% efficiency, at 25 mg L^{-1} of cadmium, 150 mg adsorbent, and pH = 10 at 100 min, respectively. The concentration of phosphoric acid was an important variable in the adsorption rate because at higher concentrations glycosidic linkage and aryl bond in lignin will be hydrolyzed which could be attributed to the fact that the electrostatic interactions will be decreased between the cadmium and activated carbon. Results showed that cadmium adsorption isotherms fitted to Langmuir and Freundlich isotherm models. Adsorption kinetic data indicated that pseudo-first-order is the best model fitted for cadmium adsorption in ACO and pseudo-second-order for ACWS.

Keywords: Adsorption; Cadmium; Activated carbon; Walnut shell; Ox tongue leftover; Water

1. Introduction

Heavy metals are considered as one of main pollutants in the environment because they have significant impacts on ecological quality [1]. Heavy metal pollution affects the food productivity and quality and the quality of atmosphere and water which threatens the animal and human health [2]. The transfer of heavy metals from the atmosphere to soil and plants occurs through dust, total shedding and gaseous or adsorption processes [3]. In general, these elements of human activities cause environmental pollution [4]. Metal contaminants include Pb, Cr, Hg, U, Se, Zn, As, Ca, Au, Ag, Cu, and Ni. Excessive presence of

* Corresponding author.

these metals in the aquatic environment could potentially damage the physiology of the human body and other biological systems [5]. In recent years, cadmium has received far more attention as one of the most toxic heavy metal. It is potentially a dangerous element for human health [6]. The natural concentration of this element in soil is between 0.01 and 2 mg/kg and the maximum allowable concentration in drinking water according to the standards of World Health Organization is less than 0.005 mg L^{-1}. The metal is also toxic at very low concentrations and causes anemia, bone fragility, kidney and nerve disorders [7]. Accordingly, many studies have been done for studying the removal of heavy metals. These studies showed that heavy metal ions could be typically removed from aqueous media by chemical deposition, ion exchange, solvent extraction, chemical oxidation and reduction reactions, reverse osmosis, filtration, and various resins. The main disadvantage of these methods includes producing high volume of sludge where its disposal and control is a problem, being relatively expensive and inefficient, especially for low concentrations of metals. Therefore, a cost-effective and environmental friendly technology is required to be employed to remove heavy metals from wastewater [8].

Adsorption using activated carbon is the most common method, but this may have some limitations such as being expensive, particularly if proper raw materials are not available and therefore carbon has to be entered the process. Activated carbon has high adsorption properties, high porosity and the presence of functional groups on the surface [9]. Environmental risks from water pollution and subsequently demand for activated carbon has increased significantly as a cleaning agent in purification processes worldwide [10]. Activated carbon can be produced from coal, wood, nut shells and agricultural waste among which agricultural products are now widely used for carbon production due to their availability in large quantities and low cost [11,12]. Due to the inherent hardness of these plants' woods, a good substrate for producing activated carbon from the waste of these plants is provided. For such process, materials with high carbon and low organic matter have the best performance. The advantage of these methods is the existence of an economical and environmental friendly technology for treatment of heavy metals from wastewater. Recent studies have suggested that the impregnation of nanoparticles, steam or nitrogen flow, microwaves, and magnetic modification methods can effectively modify the chemical reactivity and physical properties of bio-sorbent surfaces [13,14]. Besides, other methods such as activation with chemicals have also been recommended [15]. But so far, activated carbons extracted from walnut shell (ACWS) and ox tongue leftover (ACO), which are abundant in nature, have not been used to remove heavy metals from water. Investigating the activation of the plant residues at different temperatures and acid concentrations can also help to reduce costs and water pollution.

In this research, due to the structure and high access to ACWS and ACO, the effect of activated carbon adopted from these leftovers was compared to each other as an adsorbent for removing the cadmium metal in an aqueous solution. Also, carbon activation methods and its effect on the efficiency of prepared carbon in removing heavy metals from aqueous solutions was evaluated. Parameters such as feedstocks and pyrolysis condition, pH, cation exchange capacity, adsorbent dosage, cadmium heavy metal initial concentration and contact time, were investigated. While the Langmuir and Freundlich and models as well as pseudo-first model and pseudo-second models were used to analyze the adsorption isotherm data.

2. Material and methods

2.1. Chemicals and reagents

Walnut shell and ox tongue leftover were obtained from selling source in Zanjan, Iran. Phosphoric acid was purchased from Sigma-Aldrich, Spain. Also cadmium nitrate salt was purchased from Merck, Germany. All other chemicals were of analytical grade, commercially available and used without further purification.

2.2. Carbon preparation

Walnut shell and ox tongue leftover were obtained from selling source, in Zanjan, Iran. Then, they were rinsed with water to clean redundant materials such as soil and sand. The washed sample was dried facing the sun for 2 d. Carbonaceous materials were changed into charcoal for 2 h at 600°C in a low oxygen concentration.

2.3. Activated carbon

The prepared carbon was saturated with 20%, 40%, 60% and 80% concentrations of phosphoric acid respectively, and kept at 120°C for 24 h. In the next stage, it was heated at 500°C and 700°C for 2 h. After activation, the sample was washed several times with deionized water to remove excess phosphoric acid. The adsorbents were dried at 120°C for 24 h and then used in the experiments [16].

2.4. Adsorption experiments

All adsorption experiments were performed in batch mode. In model one, activated carbon (25–150 mg) was added to a 30 mL cadmium solution (25–200 mg L^{-1}) in 30 mL flasks and was shacked for (10–100 min) at room temperature, pH (2–10) and constant speed of 100 rpm. Then the mixture was filtered and the treated samples were analyzed to estimate the adsorption capacity for removing cadmium. To investigate particular effect of each variable, one variable was changed while others were kept constant [17].

The detection of the cadmium concentration in the samples was done by atomic absorption spectroscopy (AAS).

2.5. Characterization of the activated carbon samples

The concentration of cadmium in solutions was measured using atomic absorption spectroscopy (AAS, Analytik Jena novAA 350 series) equipped with a hollow-cathode lamp (HCLs) as a light source. The limit of detection (LOD) and the limit of quantification (LOQ) of AAS device were 1 and 140 μg L^{-1}, respectively. The Fourier-transform infrared spectroscopy (FT-IR) were recorded using a Perkin Elmer-Spectrum 65 device at 4,000 and 400 cm^{-1} from KBr

pellets for determining surface functional groups of raw materials and produced activated carbon samples. Field-emission scanning electron microscopy (FE-SEM) images were taken by FE-SEM on LEO 1455 VP equipped with an energy-dispersive X-ray spectroscopy (EDX) apparatus for analyzing the surface morphology of produced activated carbon samples and identifying the elemental surface composition. The structure of adsorbents was investigated by recording X-ray powder diffraction (XRD) patterns with a SIEMENS D5000 X-ray diffractometer using Cu-Kα radiation (λ = 1.54059 Å) over the range of $10° < 2\theta < 90°$.

2.6. Equation of elimination percentage

The elimination efficiency was calculated through Eq. (1):

$$\%R = \frac{\left(C_i - C_t\right)}{C_i} \times 100 \tag{1}$$

where $\%R$ is removal percentage, C_i is the initial concentration of metal in aqueous solution (mg L^{-1}), and C_t is the secondary concentration of metal in aqueous solution (mg L^{-1}).

2.7. Adsorption equation

The adsorption process was defined by Eq. (2):

$$Q_t = \frac{V\left(C_i - C_t\right)}{m} \tag{2}$$

where Q_t is the amount of adsorbed metal per unit mass of adsorbent (mg g^{-1}), C_i is the initial concentration of metal in aqueous solution (mg L^{-1}), C_t is the secondary concentration of metal in aqueous solution (mg L^{-1}), t is the amount of time after adding the adsorbent, V is the volume of the aqueous solution (l), and m is the adsorbent mass (g) [18].

2.8. Adsorption isotherms

The adsorption isotherms describe the distribution of adsorbate between liquid and solid phases in the equilibrium condition. The adsorption equilibrium data were fitted to the Langmuir (1) and Freundlich isotherms which are shown as Eqs. (3) and (4), respectively.

$$q_e = q_{\max} \frac{bC_e}{1 + bC_e} \tag{3}$$

$$q_e = K_F C_e^{1/n} \tag{4}$$

where q_e is the equilibrium adsorption (mg g^{-1}), q_m is the maximum adsorption capacity (mg g^{-1}), b is the adsorption equilibrium constant (g mg^{-1}) showing the characteristic of the affinity between adsorbent and adsorbate. K_F and q_m can be obtained by linear regression of (C_e/q_e) vs. C_e data and where K_F is the Freundlich adsorption constant [(g mg)$^{-1/n}$]. This is an indicator of the adsorption capacity, while n refers to the adsorption tendency [19].

2.9. Adsorption kinetic

The adsorption kinetic data for cadmium on the prepared adsorbents were fitted using the most frequently used kinetic models reported by Lagergren and Ho that led to a pseudo-first-order adsorption rate (5) and a pseudo-second-order adsorption rate (6).

$$\ln\left(q_e - q_t\right) = \ln q_e - k_1 t \tag{5}$$

$$q_t = \frac{K_2 q_e^2 t}{1 + k_2 q_e t} \tag{6}$$

where q_e (mg g^{-1}) is the adsorption capacity at equilibrium, q_t in (mg g^{-1}) is the adsorption capacity at a time t (min), k_1 (min^{-1}) is the pseudo-first-order rate constant, and k_2 (g mg^{-1} min^{-1}) is the pseudo-second-order rate constant.

3. Results and discussion

3.1. Adsorption mechanism

Cadmium ions' sorption process can be divided into two forms: physical and chemical adsorption. Physical sorption is capable of forming a multilayer cadmium sorption process that creates great adsorption capacity while chemical sorption is limited to monolayer adsorption. Physical sorption process happens when cadmium ions are electrostatically across (weak Van der Waals forces) the surface of the activated carbons. While chemical sorption process happens between the cadmium ions and the surface of the activated carbon by chemical bonding or electron transfer. In chemical sorption the functional groups on the adsorbent surface such as carbonyl, hydroxide groups, etc. are able to bind to cadmium ions by substituting hydrogen ions with cadmium ions or by donating electron pairs. Comparing the structure of ACWS and ACO, it can be inferred that the structure of ACWS has more lignin, and for this reason, the electrostatic interactions (physical sorption process) will be more desirable for cadmium adsorption on ACWS.

3.2. Characterization

3.2.1. Surface areas and pore size distributions

The nitrogen adsorption–desorption isotherms of the activated carbons ACWS and ACO prepared are shown in Fig. 1. The activation experiments have been performed at two temperatures 500°C and 700°C. The results indicate a mixed type (i.e., isotherms I and IV) according to IUPAC classification reflecting the domination of mixture of microporous and mesoporous materials in the structure. The initial part is by applying significant adsorption at low relative pressures. This is the isotherm of type I which corresponds to adsorption in micropores. The isotherm is of type IV in relative pressures with monolayer–multilayer adsorption by doing the process in narrow pores. Result showed nitrogen uptake reduction with the increasing of activation temperature from 500°C to 700°C. This indicates surface area and micropore volume reduction which may be due to shrinkage in the carbon structure and deterioration of porous structure. The Brunauer–Emmett–Teller

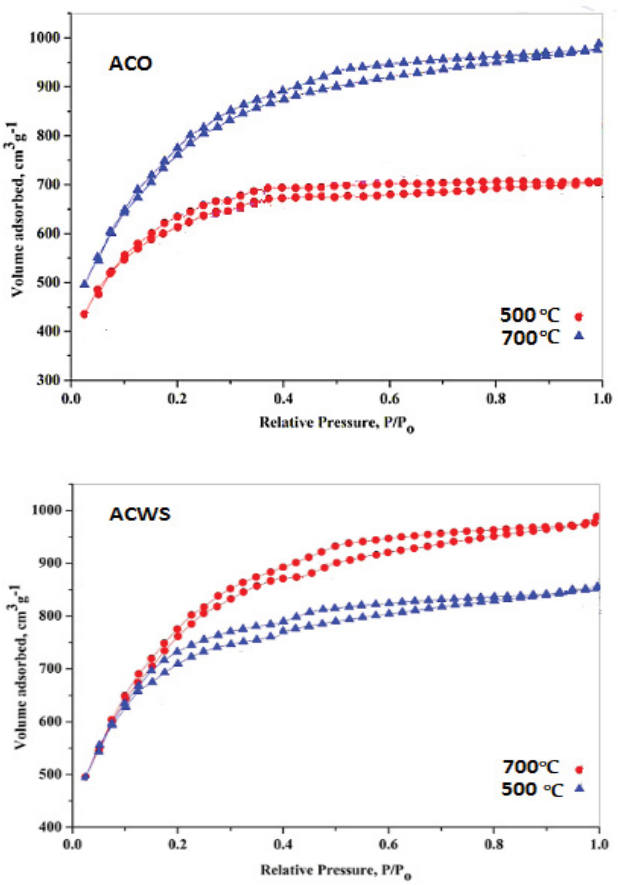

Fig. 1. Isotherms of nitrogen for ACO and ACWS.

surface area ACWS at 500°C and 700°C is 2,450.18 and 2,110.47 m^2 g^{-1}, respectively, and for ACO at 500°C and 700°C is 1,899.3 and 1,684.4 m^2 g^{-1}, respectively.

3.2.2. XRD pattern

XRD patterns of synthesized walnut shell and ox tongue leftover after activation are shown in Fig. 2. The diffraction peak at 2θ = 45.5° and 52.3° corresponds to the crystallinity phase of ACWS. This spectrum showed four peaks which corresponds to the tetragonal phase at 2θ = 28.2°, 34.5°, 54° and 63° for the synthesized ACWS. Based on the XRD patterns, ACWS depicted diffraction peaks at 24.3° and 46.5° which could be traced to carbon phase as the graphite structure. On the other hand, there are two wide diffraction backgrounds corresponding to 2θ = 25° and 2θ = 43° in ACO's pattern which could be traced to low crystallinity.

3.2.3. Surface morphology

FE-SEM images of ACWS and ACO are shown in Fig. 3. A comparison between FE-SEM images of activated carbon before and after synthetization indicated that phosphoric acid generated highly porous and sheet structure. Porous structure was formed as a result of generation of volatile matters after carbonization. The ACO is constructed from closed pores due to a geometry of sheet layer which is due

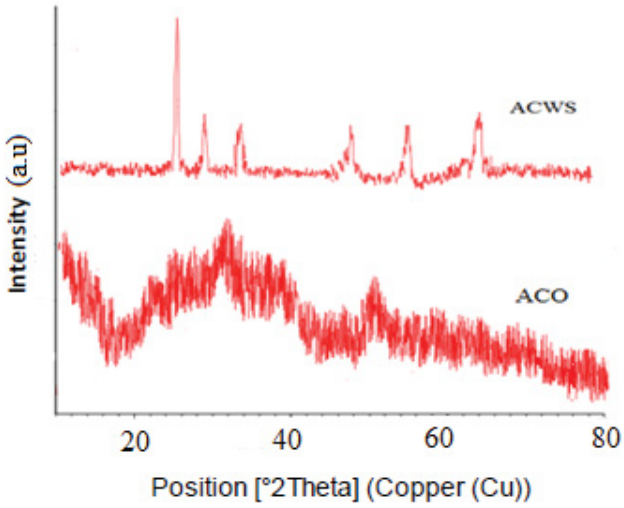

Fig. 2. XRD patterns of synthesized ACWS and ACO.

to the fact that increasing carbon-phosphoric acid reaction, the glyosidic linkage and aryl bond in lignin will be hydrolyzed by H_3PO_4. On the other hand, ACWS has open pore in which the geometry structure is regular sheets. This structure is due to the presence of lignin in the hard shell of the walnut. Fig. 4 shows EDX for the elemental analysis of ACWS and ACO. It indicates that removal efficiency in activated carbon is 67.34% and 65.73% in ACWS and ACO, respectively. These analyses also show the presence of low concentrations of Mg, Cl, Fe and, for example, elements.

3.2.4. FT-IR spectra

The FT-IR spectra of ACWS and ACO are shown in Fig. 5. ACWS and ACO indicated wide absorption bands at 3,420 cm^{-1} which represents the stretching vibration of O–H in hydroxyl groups and adsorbed water. The band at 1,550–1,700 cm^{-1} is usually assigned to C=O stretch in aldehydes, lactones or carboxyl groups. The weak intensity of this peak suggests that it may be correlated to thermal instability of aldehyde and ketone groups at high temperature and that is the reason for ACWS and ACO containing small amounts of carboxyl groups. The spectra for ACWS and ACO are indicative of a strong band at 1,600–1,560 cm^{-1} due to aromatic ring stretching vibrations (C=C) enhanced by polar functional groups. The 1,100–1,250 cm^{-1} adsorption band is attributed to the vibration of the C=O group in lactones where is usually found in oxidized carbons and carbons activated by phosphoric acid. Peaks at 766 cm^{-1} shows the formation of bending vibration from –C (triple bond). Also, C–H peaks at 766 cm^{-1} shows formation bending vibration from –C (triple bond) which is from alkynes and corresponds to C–O–C stretching (ester, ether and phenol) and out-of-plane bending in benzene derivatives.

3.3. Optimal conditions

3.3.1. Effect of pH

pH is an important parameter for sorption of metal ions from solution due to its effects on the functional

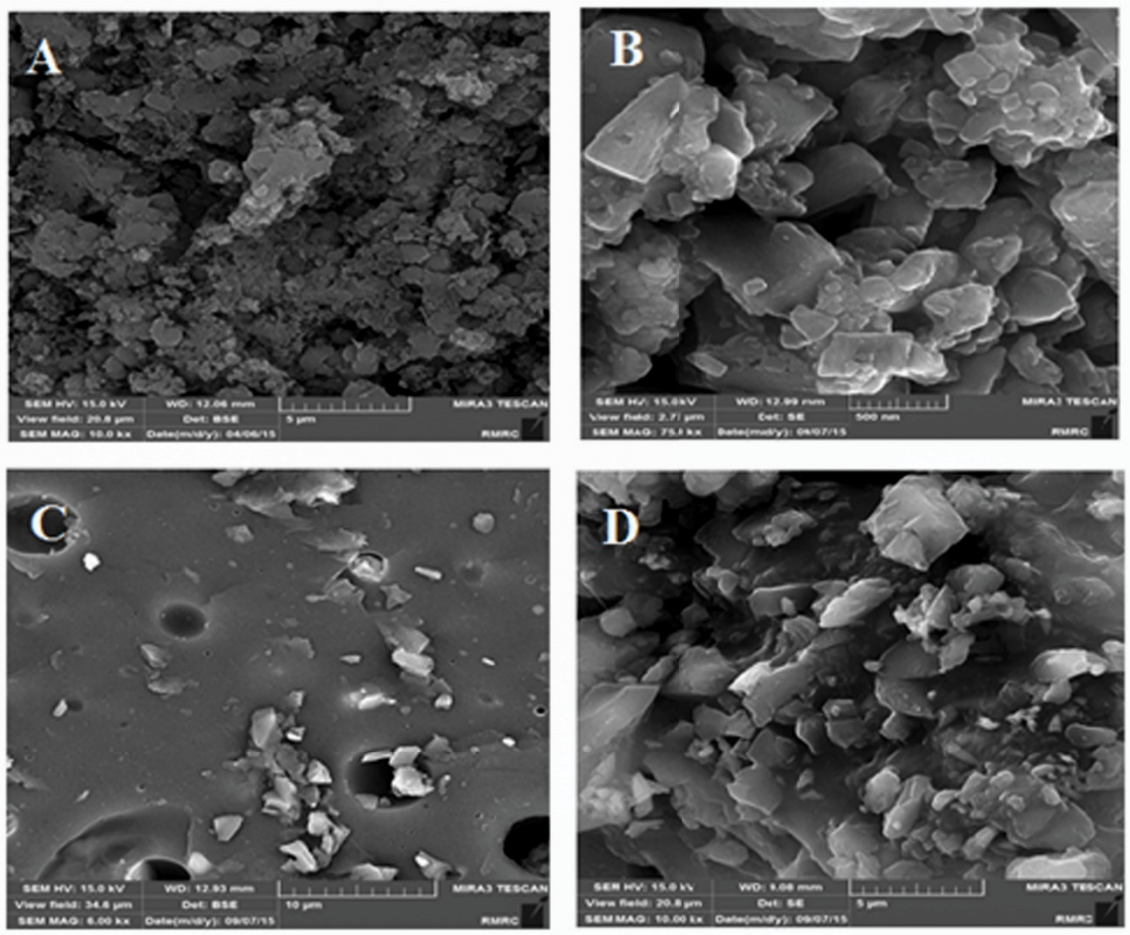

Fig. 3. FE-SEM images of ACWS (A, B) and ACO (C, D) before and after of the synthesized activated carbons.

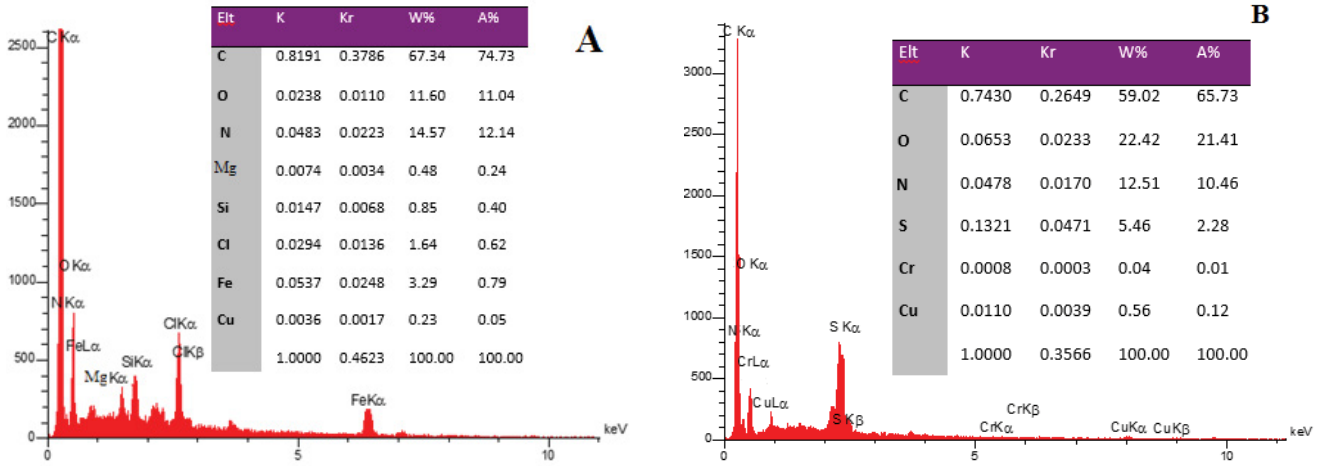

Fig. 4. EDX analysis of ACWS (A) and ACO (B).

groups such as carboxyl and hydroxyl groups on adsorbent surface. In addition, pH determines the ionic state of metals and the amount of charge on the adsorbent surface, which will also affect the reaction between the adsorbent and metal ions. Adsorption of cationic materials will be increased at higher pH because the presence of functional groups creates negative charge at the surface of activated carbon. By increasing pH, the percentage of cadmium uptake also rose so that the highest and the lowest percentage of cadmium removal were observed at pH = 10

and pH = 2, respectively (Fig. 6), it is because hydrogen ions at acidic pH would fiercely compete the reaction with metal ions in adsorption sites. Kumar et al. [2] found that the optimum pH of rice paddy carbon modified with sodium bicarbonate as adsorbent in removal of cadmium was equal to 9. The interaction effects of adsorbent type and pH of equilibrium solutions on the percentage of cadmium removal from aqueous solutions show that ACWS prepared with 20% phosphoric acid at pH 10 had a higher removal efficiency than ACO with 90.66% and 89.33% from aqueous solution at 500°C and 700°C, respectively (Fig. 7). In addition, comparing carbon activation temperatures (500°C and 700°C) and concentration of phosphoric acid (20%–80%), activated carbon produced at 500°C along with 20% phosphoric acid had a higher efficiency for cadmium removal (Fig. 8A and B). The reason is that at higher temperatures and in acidic conditions, the aryl lignin bonds are cleavage, the carbon plates are stacked, and the pores in the carbon would be destroyed. Generally, in comparing ACWS and ACO which have been synthesized in different percentages of phosphoric acid at 500°C and 700°C, ACWS showed a better performance at different pH levels (Fig. 9A and B).

One of the most important factors determining the removal efficiency is the electric charge of the adsorbent surface. Zero-potential (pH_{PZC}) indicates at which pH the adsorbent surface has a neutral or zero electric charge. When the pH of the solution is less than pH_{PZC}, the adsorbent surface in the solution has a positive electric charge and when it is higher than pH_{PZC}, the adsorbent surface has a negative charge. Solid addition method was used to determine the pH of zeta potential. The results are shown in Fig. 10. Based on the obtained information, it was determined that at pH = 7.1, the adsorbent surface has an electric charge equal to zero. Due to the fact that the surface charge of cadmium in water is positive, the best pH for the adsorption of this ion by the adsorbent is at a pH higher than the zeta potential, where the electric charge is negative.

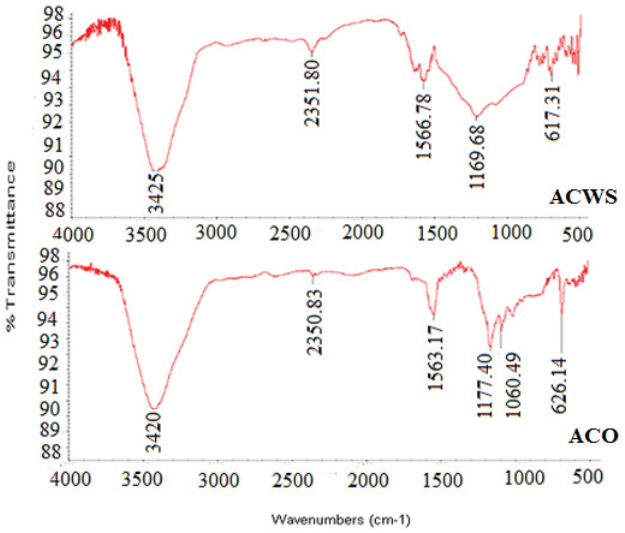

Fig. 5. FT-IR spectra of ACWS and ACO.

3.3.2. *Effect of adsorbent dose*

The dependence of cadmium adsorption on activated carbon dosage is indicated in Fig. 11A and B. The higher adsorbent dosage in the solution creates more exchangeable active sites for adsorption process. Comparing activated carbons in terms of the effect of different percentages of phosphoric acid and activation temperature showed that ACWS prepared with 20% phosphoric acid at 500°C with the adsorbent amount of 150 mg had the highest cadmium removal efficiency (Figs. 12 and 13A & B). The interaction effects of adsorbent type and adsorbent dosage of equilibrium solutions on cadmium removal from aqueous solutions showed that ACWS had the best performance with 44.26% removal (Fig. 14). A similar behavior of adsorption efficiency of cadmium was investigated by activated carbon of bagasse pulp. The results showed that for different amounts of adsorbent dose, by increasing adsorbent

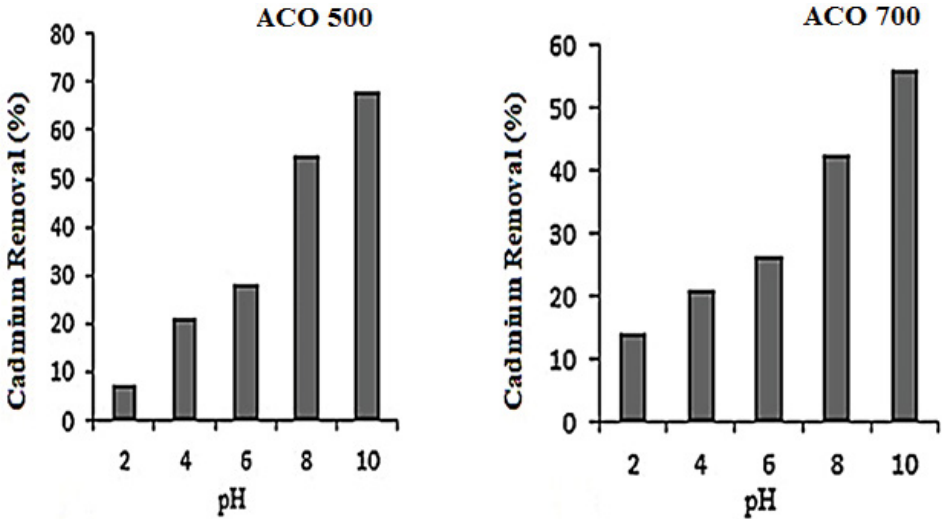

Fig. 6. Effect of pH on removal of cadmium with ACO 500 and ACO 700; [Operating conditions of AAS: HCLs, *C*: 3.5 mA, wavelength: 228.8 nm, spectral band pass: 0.5 nm, LOD: 1 μg L^{-1}, LOQ: 140 μg L^{-1}].

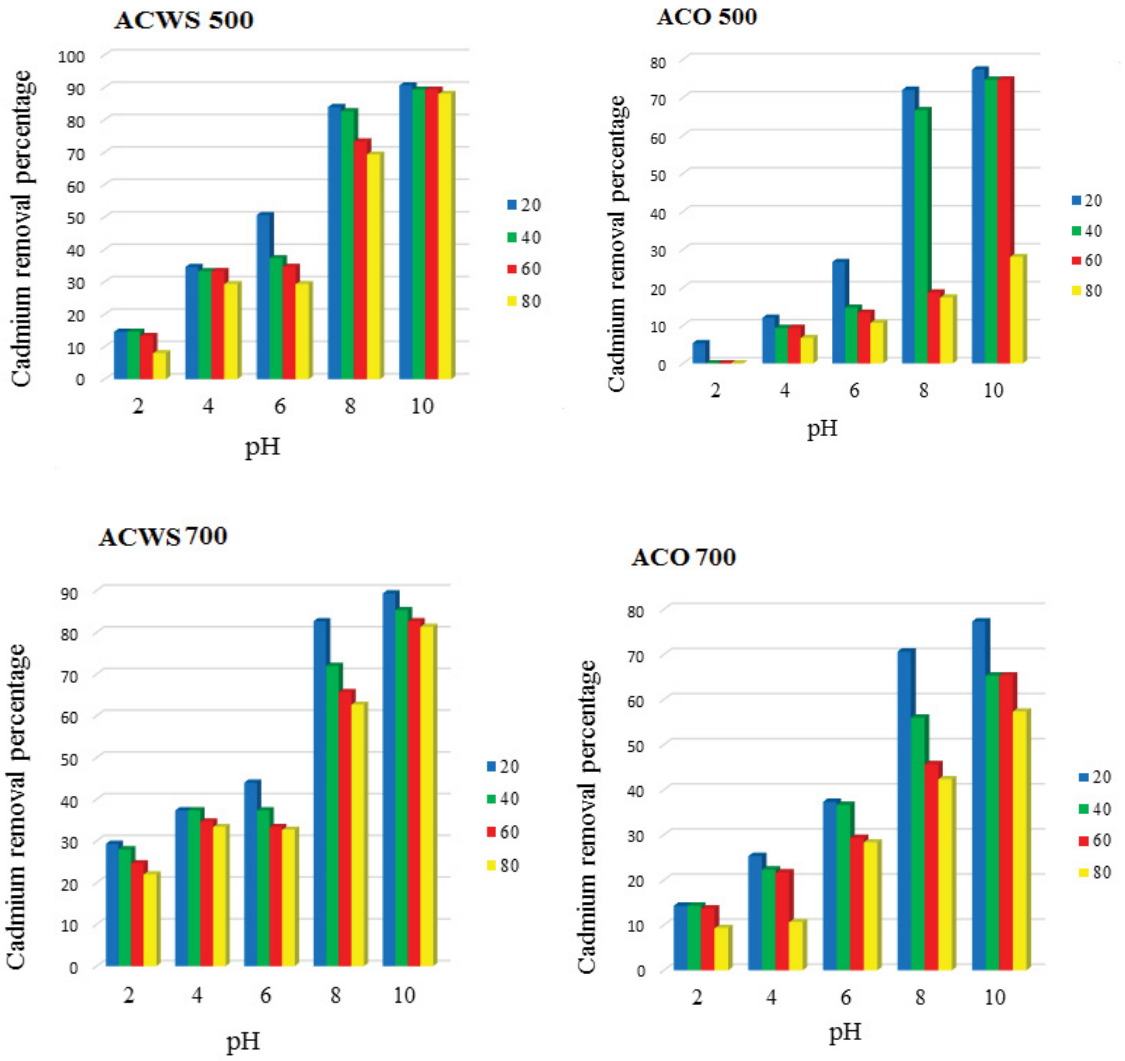

Fig. 7. Comparison of the mean interaction of ACWS and ACO adsorbents activated with different concentrations of phosphoric acid (20%, 40%, 60% and 80%) and pH of equilibrium solutions on the percentage of cadmium removed at 500°C and 700°C; [Operating conditions of AAS: HCLs, *C*: 3.5 mA, wavelength: 228.8 nm, spectral band pass: 0.5 nm, LOD: 1 μg L^{-1}, LOQ: 140 μg L^{-1}].

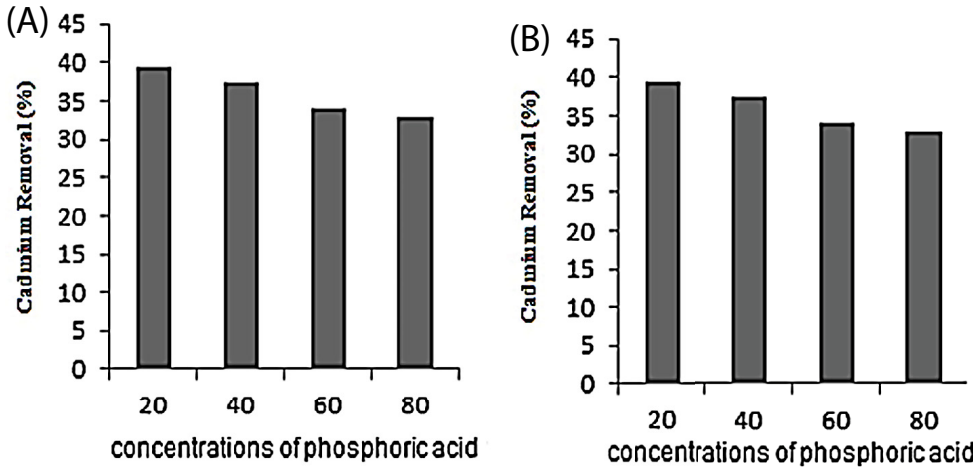

Fig. 8. Effect of concentration of H_3PO_4 on adsorption of cadmium at 500°C (A) and 700°C (B); [Operating conditions of AAS: HCLs, *C*: 3.5 mA, wavelength: 228.8 nm, spectral band pass: 0.5 nm, LOD: 1 μg L^{-1}, LOQ: 140 μg L^{-1}].

dose the adsorption efficiency rose because the higher surface area of activated carbon would provide more adsorption surface sites [14].

3.3.3. Effect of initial cadmium ions' concentration

The initial cadmium ions' concentration causes a significant driving force to overcome all the mass transfer resistance between the aqueous solution and solid phases as well as enhancing the interaction between cadmium ions and activated carbon surface. In general, the removal rate of cadmium declined with increasing cadmium concentration because with a constant amount of adsorbent, due to the rapid occupation of adsorption sites which was related to high concentrations, the removal percentage decreased. The highest and lowest of cadmium removal percent in aqueous solutions were observed for concentrations equal to 25 and 200 mg L^{-1}, respectively (Fig. 15A and B). The interaction effects of adsorbent type and different concentrations of soluble cadmium on cadmium removal from aqueous solutions showed that activated carbon prepared from walnut shell with 20% phosphoric acid and cadmium content of 25 mg L^{-1} had the highest purification rate with 88.66% of cadmium removal (Fig. 16). Luo et al. [13] studied the effect of cadmium input concentration in the removal process by activated carbon made from paddy husk.

3.3.4. Effect of contact time

Fig. 17A and B indicate the influence of contact time on the adsorption capacity of cadmium. The sorption process was accelerated within the first 10 min and this may be attributed to the available empty adsorption sites at the initial phase of cadmium sorption. The rate of cadmium removal from the aqueous solution increased as the time passed. The highest and lowest cadmium removal were reached at contact time equal to 100 and 10 min, respectively. The interaction effects of adsorbent type and its

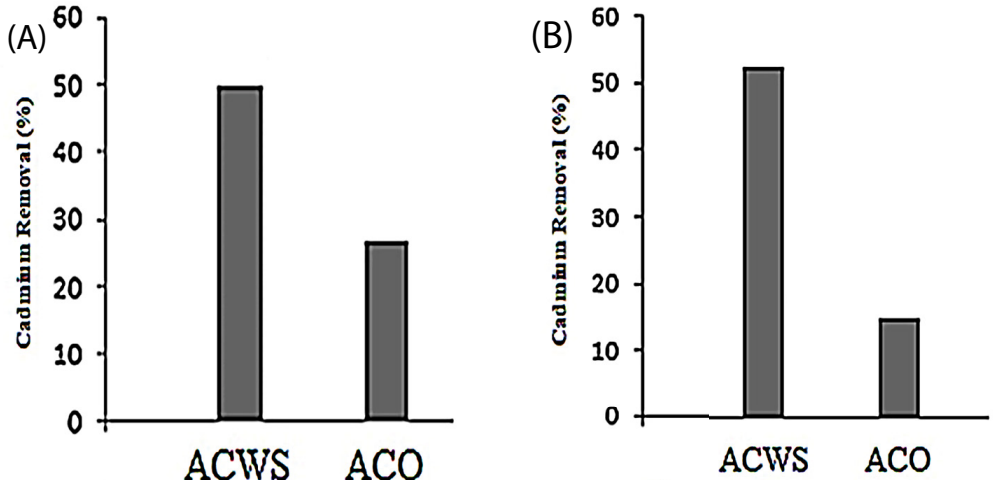

Fig. 9. Comparison of the mean effect of ACWS and ACO at 500°C (A) and 700°C (B) on the percentage of cadmium removed from the aqueous solution at different pH; [Operating conditions of AAS: HCLs, *C*: 3.5 mA, wavelength: 228.8 nm, spectral band pass: 0.5 nm, LOD: 1 μg L^{-1}, LOQ: 140 μg L^{-1}].

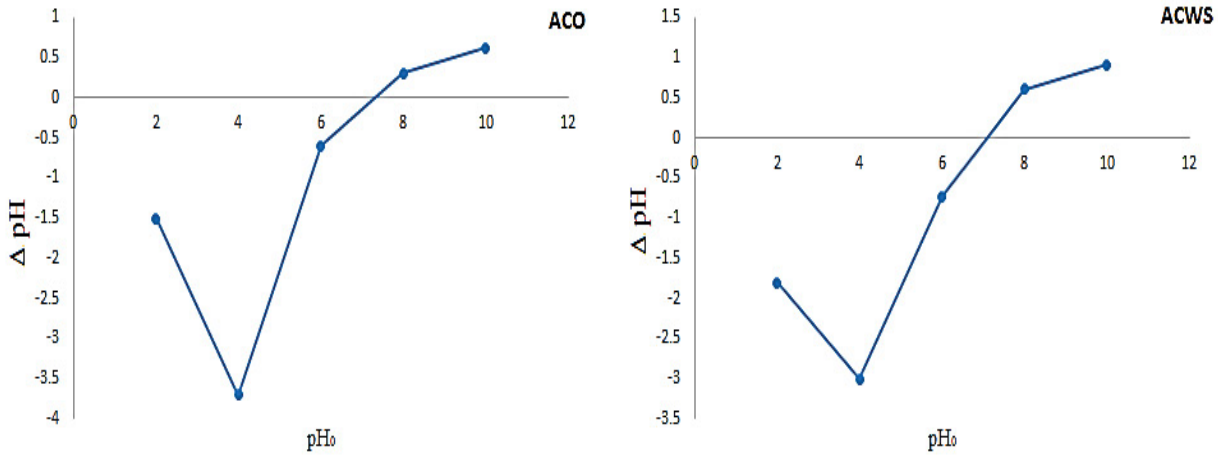

Fig. 10. Point of zero charge of the ACO and ACWS; [Operating conditions: *M*: 1 mg, *T*: 24 h, *T*: 25°C].

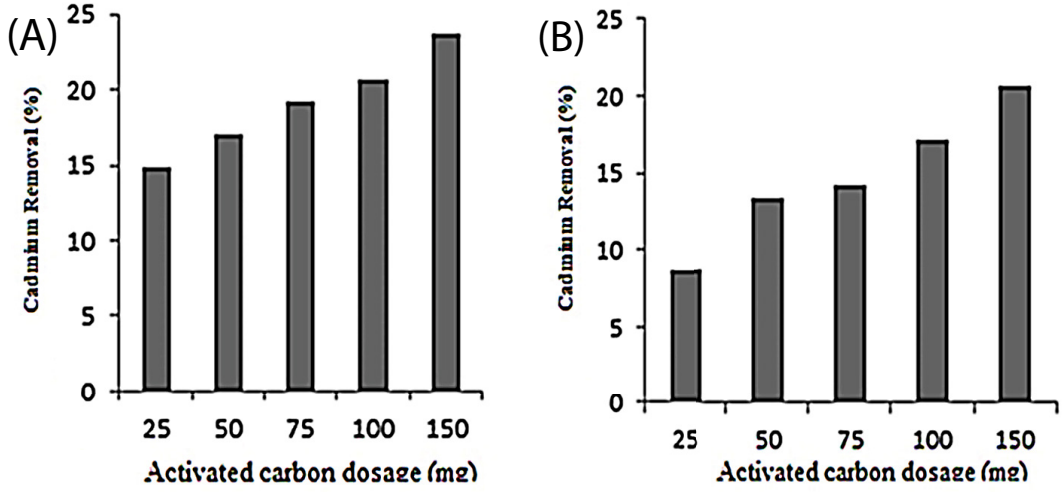

Fig. 11. Effect of adsorbent dosage on adsorption of cadmium at 500°C (A) and 700°C (B); [Operating conditions of AAS: HCLs, *C*: 3.5 mA, wavelength: 228.8 nm, spectral band pass: 0.5 nm, LOD: 1 μg L^{-1}, LOQ: 140 μg L^{-1}].

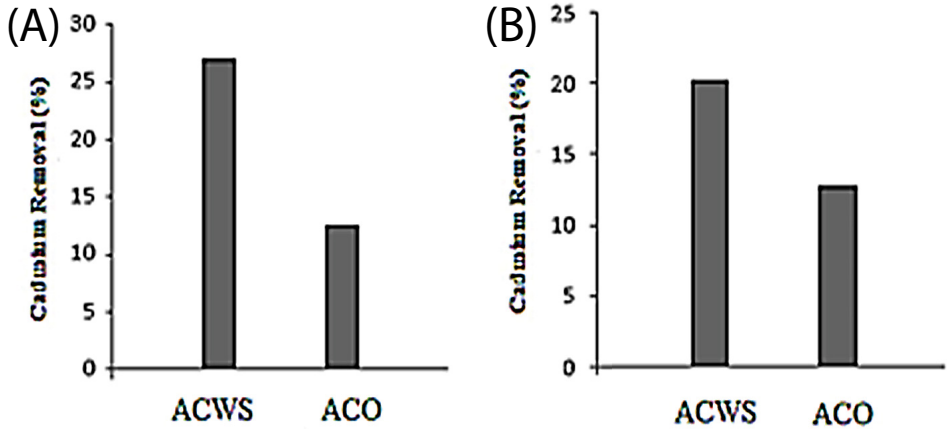

Fig. 12. Comparison of the mean effect of ACWS and ACO at 500°C (A) and 700°C (B) on the percentage of cadmium removed from the aqueous solution at different adsorbent dosage; [Operating conditions of AAS: HCLs, *C*: 3.5 mA, wavelength: 228.8 nm, spectral band pass: 0.5 nm, LOD: 1 μg L^{-1}, LOQ: 140 μg L^{-1}].

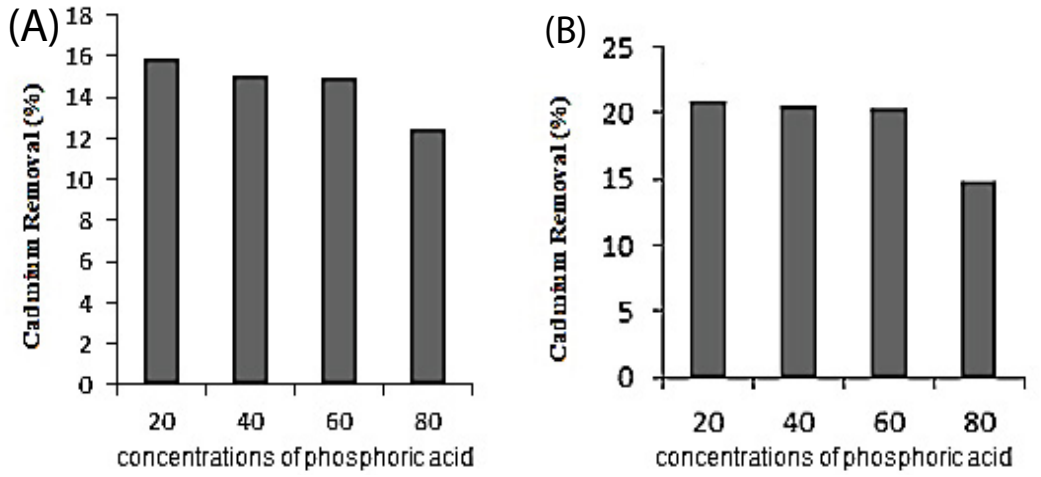

Fig. 13. Effect of concentration of H_3PO_4 on adsorption of cadmium at 500°C (A) and 700°C (B); [Operating conditions of AAS: HCLs, *C*: 3.5 mA, wavelength: 228.8 nm, spectral band pass: 0.5 nm, LOD: 1 μg L^{-1}, LOQ: 140 μg L^{-1}].

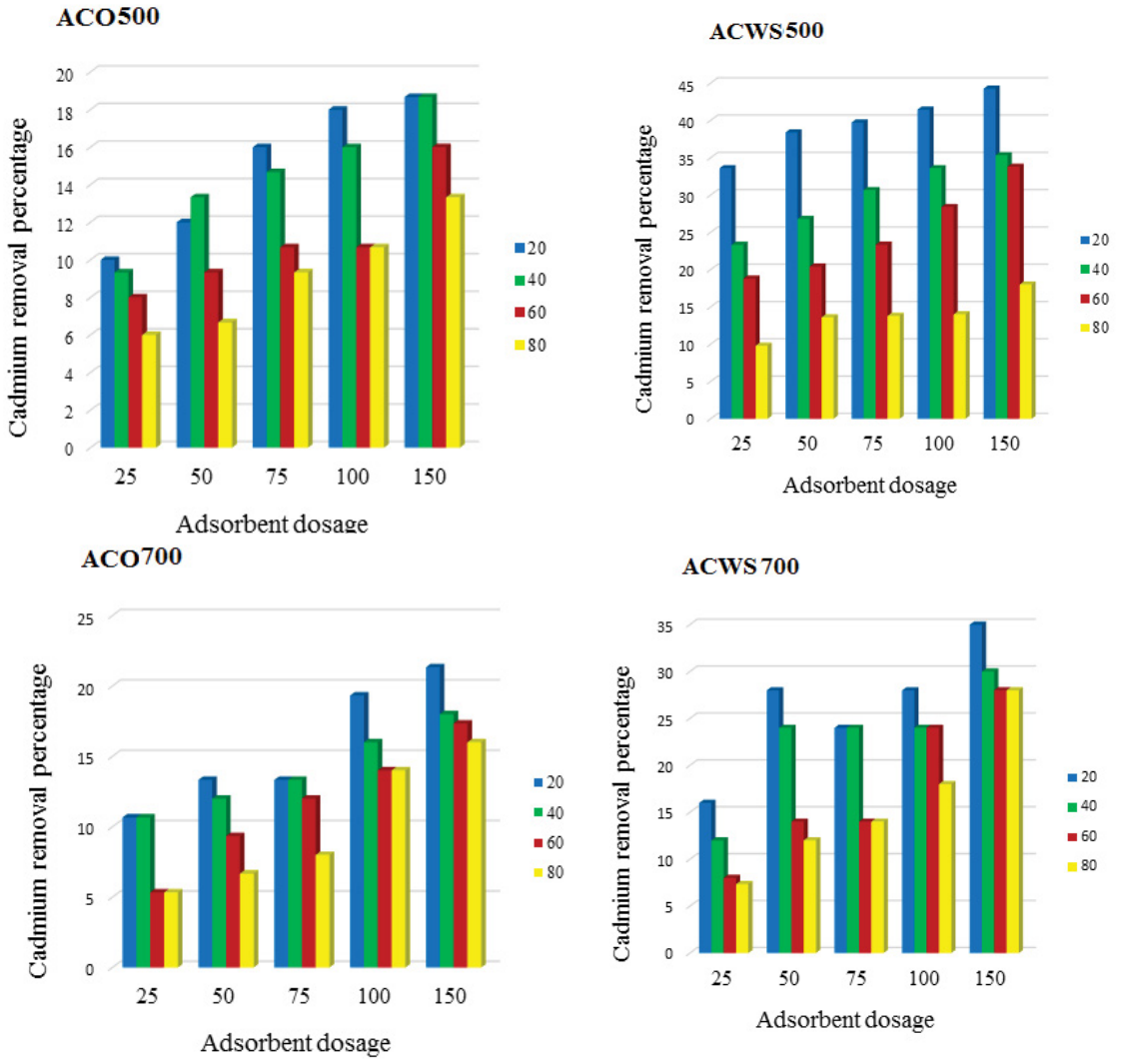

Fig. 14. Comparison of the mean interaction of ACWS and ACO adsorbents activated with different concentrations of phosphoric acid (20%, 40%, 60% and 80%) and dosage of equilibrium solutions on the percentage of cadmium removed at 500°C and 700°C; [Operating conditions of AAS: HCLs, C: 3.5 mA, wavelength: 228.8 nm, spectral band pass: 0.5 nm, LOD: 1 μg L^{-1}, LOQ: 140 μg L^{-1}].

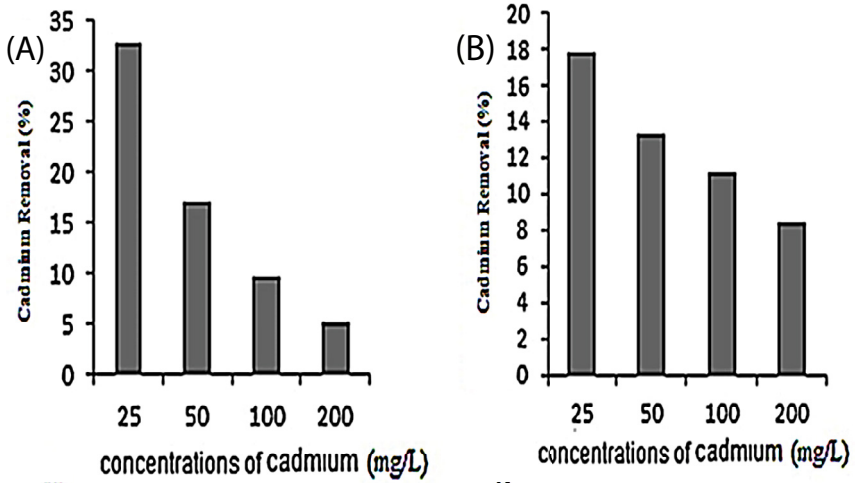

Fig. 15. Effect of concentration of cadmium on removal of cadmium at 500°C (A) and 700°C (B); [Operating conditions of AAS: HCLs, C: 3.5 mA, wavelength: 228.8 nm, spectral band pass: 0.5 nm, LOD: 1 μg L^{-1}, LOQ: 140 μg L^{-1}].

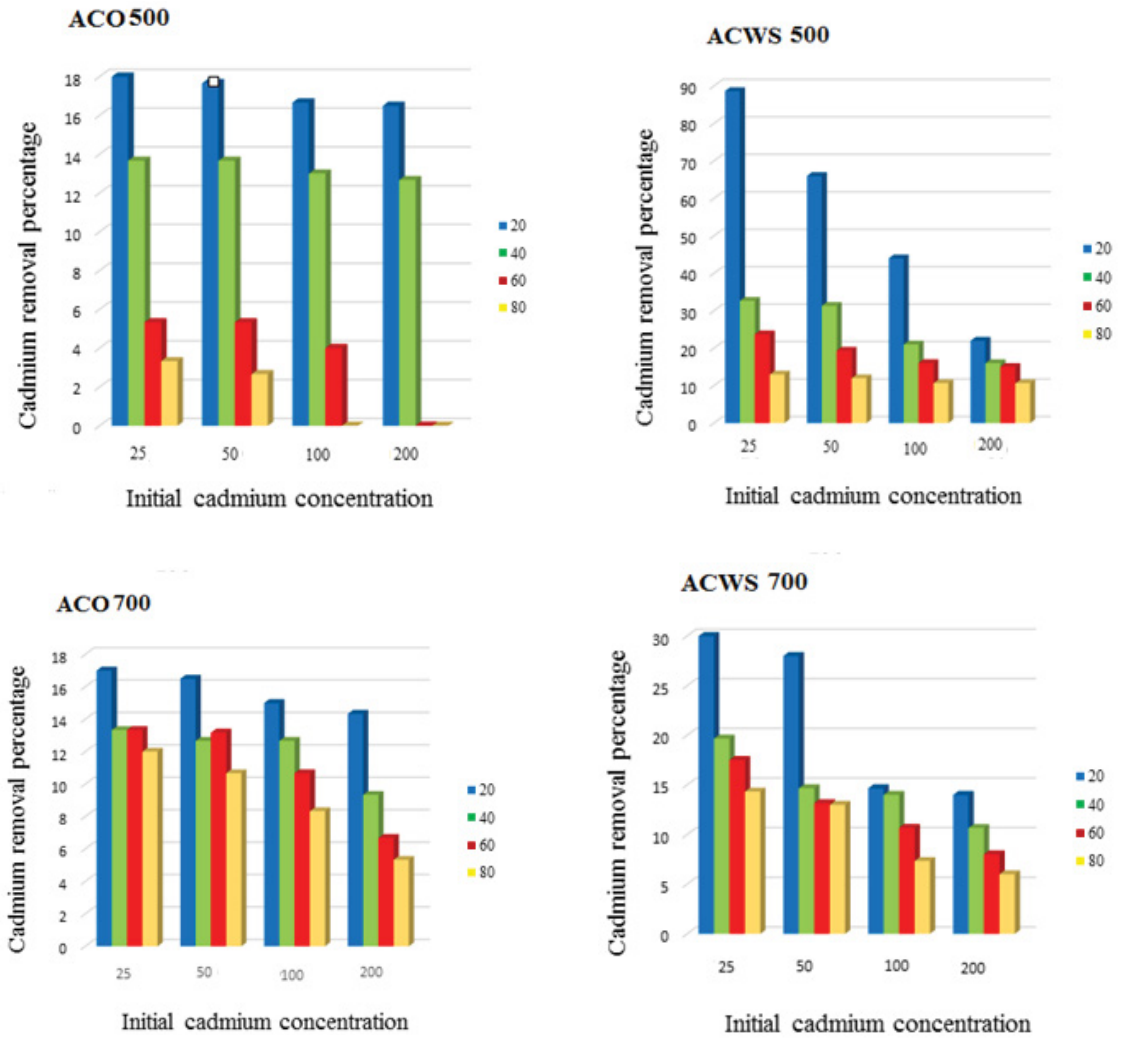

Fig. 16. Comparison of the mean interaction of ACWS and ACO adsorbents activated with different concentrations of phosphoric acid (20%, 40%, 60% and 80%) and concentration of cadmium of equilibrium solutions on the percentage of cadmium removed at 500°C and 700°C; [Operating conditions of AAS: HCLs, *C*: 3.5 mA, wavelength: 228.8 nm, spectral band pass: 0.5 nm, LOD: 1 μg L^{-1}, LOQ: 140 μg L^{-1}].

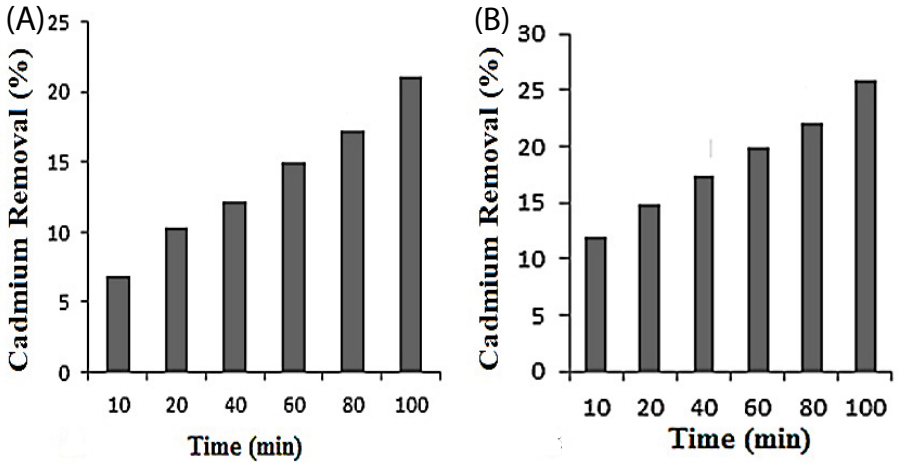

Fig. 17. Effect of contact time on adsorption of cadmium at 500°C (A) and 700°C (B); [Operating conditions of AAS: HCLs, *C*: 3.5 mA, wavelength: 228.8 nm, spectral band pass: 0.5 nm, LOD: 1 μg L^{-1}, LOQ: 140 μg L^{-1}].

contact time with the solution on cadmium removal from aqueous solutions showed that activated carbon prepared from walnut shell with a concentration of 20% phosphoric acid and a duration of a 100-min contact time had the highest cadmium removal level (44%) from aqueous solution (Fig. 18).

Table 1 demonstrates a comparative analysis of the percentage of cadmium removal using different adsorbents [20–30].

3.4. Reuse of spent adsorbent

To evaluate the performance of the adsorbent, the reaction cycle was repeated in four stages. After each absorbent run, the sample was analyzed to determine the cadmium concentration. The results are summarized in Fig. 19. The absorption capacity of cadmium was obtained after the four reaction periods of approximately 84.12 and 83.11 mg g^{-1} for ACWS and ACO, which demonstrates the stability and recyclable of the synthesized adsorbent. The slight decrease in removal efficiency may be related to the adsorption amounts of cadmium oxide on the surface of the adsorbent.

3.5. Adsorption isotherms

The adsorption isotherm illustrates how cadmium ions are partitioned between sorbet (q_e) and aqueous concentration C_e at equilibrium as a function of adsorbate concentration at room temperature (Figs. 20 and 21). The results for equilibrium adsorption of cadmium ion by ACWS and ACO are indicated in Table 2. According to the experimental results and the correlation coefficients (R^2), it could be claimed that the Langmuir and Freundlich models were the most appropriate models for cadmium adsorption by ACWS and ACO with 60% phosphoric acid at 700°C and mentioning that the monolayer

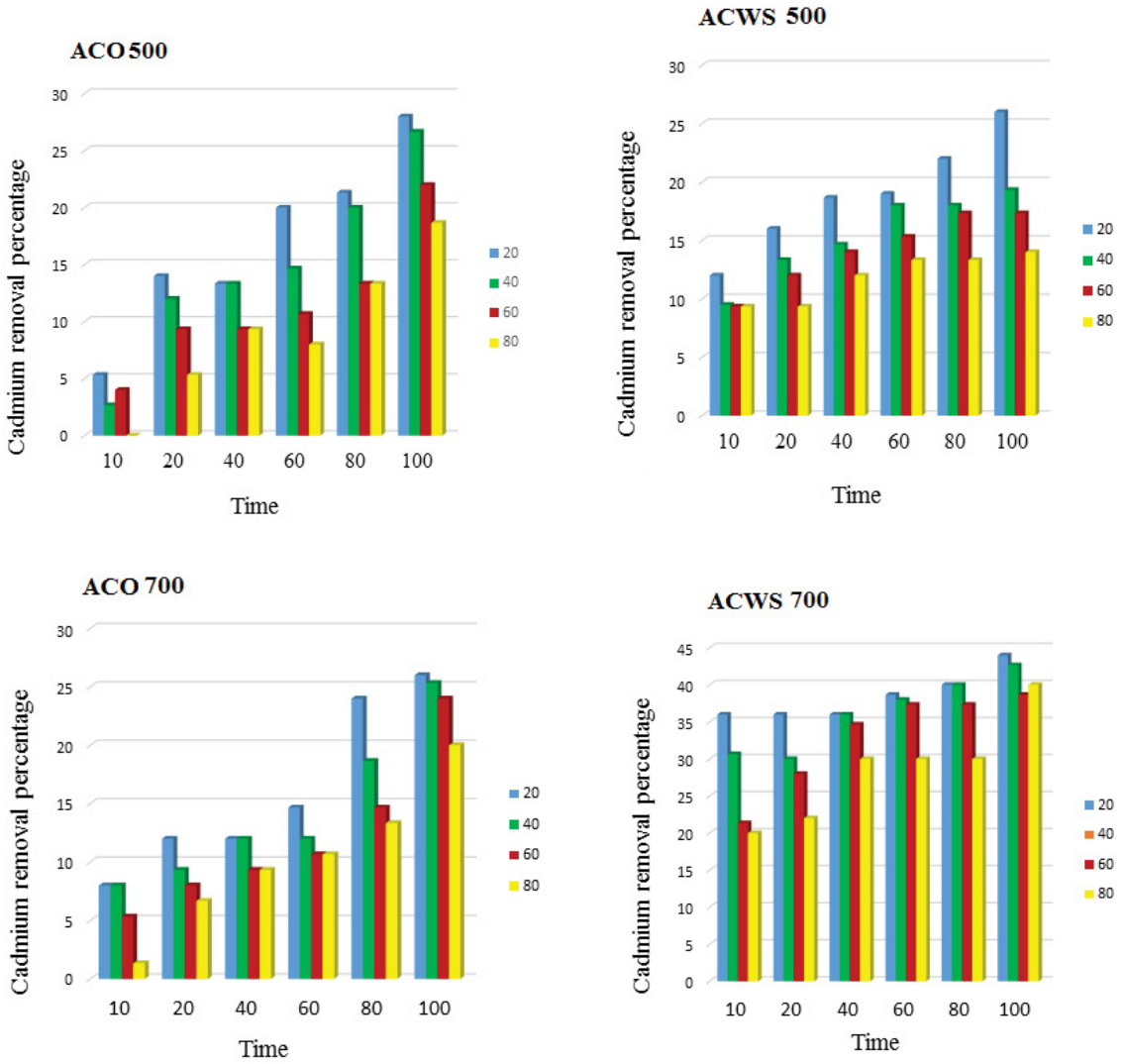

Fig. 18. Comparison of the means of interaction of adsorbent type and contact time of equilibrium solutions on the percentage of cadmium removed at 500°C and 700°C; [Operating conditions of AAS: HCLs, *C*: 3.5 mA, wavelength: 228.8 nm, spectral band pass: 0.5 nm, LOD: 1 μg L^{-1}, LOQ: 140 μg L^{-1}].

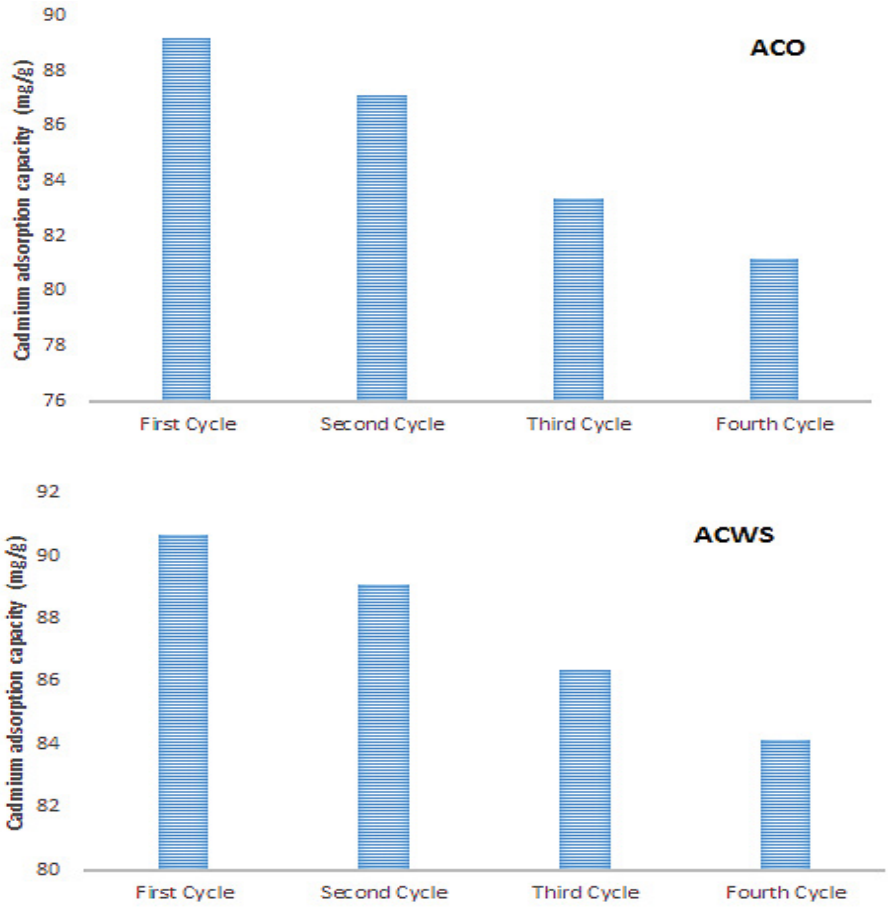

Fig. 19. Reusability profile of ACO and ACWS; [Operating conditions of AAS: HCLs, *C*: 3.5 mA, wavelength: 228.8 nm, spectral band pass: 0.5 nm, LOD: 1 μg L^{-1}, LOQ: 140 μg L^{-1}].

Table 1
Comparison of adsorption capacities for cadmium metal using different adsorbents

Source	Adsorbent	Adsorption capacity (mg g^{-1})	References
Water	ACWS	14	Present
	ACO	13.66	work
Aqueous solutions	Silica coated metal–organic frameworks	634	[20]
Aqueous solutions	PCP in PH ≤ 2	194	[21]
	PCP in PH 5–6	400	
Aqueous solutions	Pistachio shell	51.2	[22]
	Peanut shells	62.1	
	Almond shells	78.7	
Aqueous solutions	Rice husk biochar	17.8	[23]
Aqueous solutions	Lucerne biochar	6.28	[24]
Aqueous solutions	Pinecone	92.7	[25]
Water	Carboxymethyl cellulose-bridged chlorapatite nanoparticles	143.25	[26]
Aqueous solutions	Banana peel	98.4	[27]
Wastewater	GAMAAX hydrogel	259.5	[28]
Aqueous solutions	Chicken manure	10.9	[29]
Water	Magnetic carbon aerogel	143.88	[30]

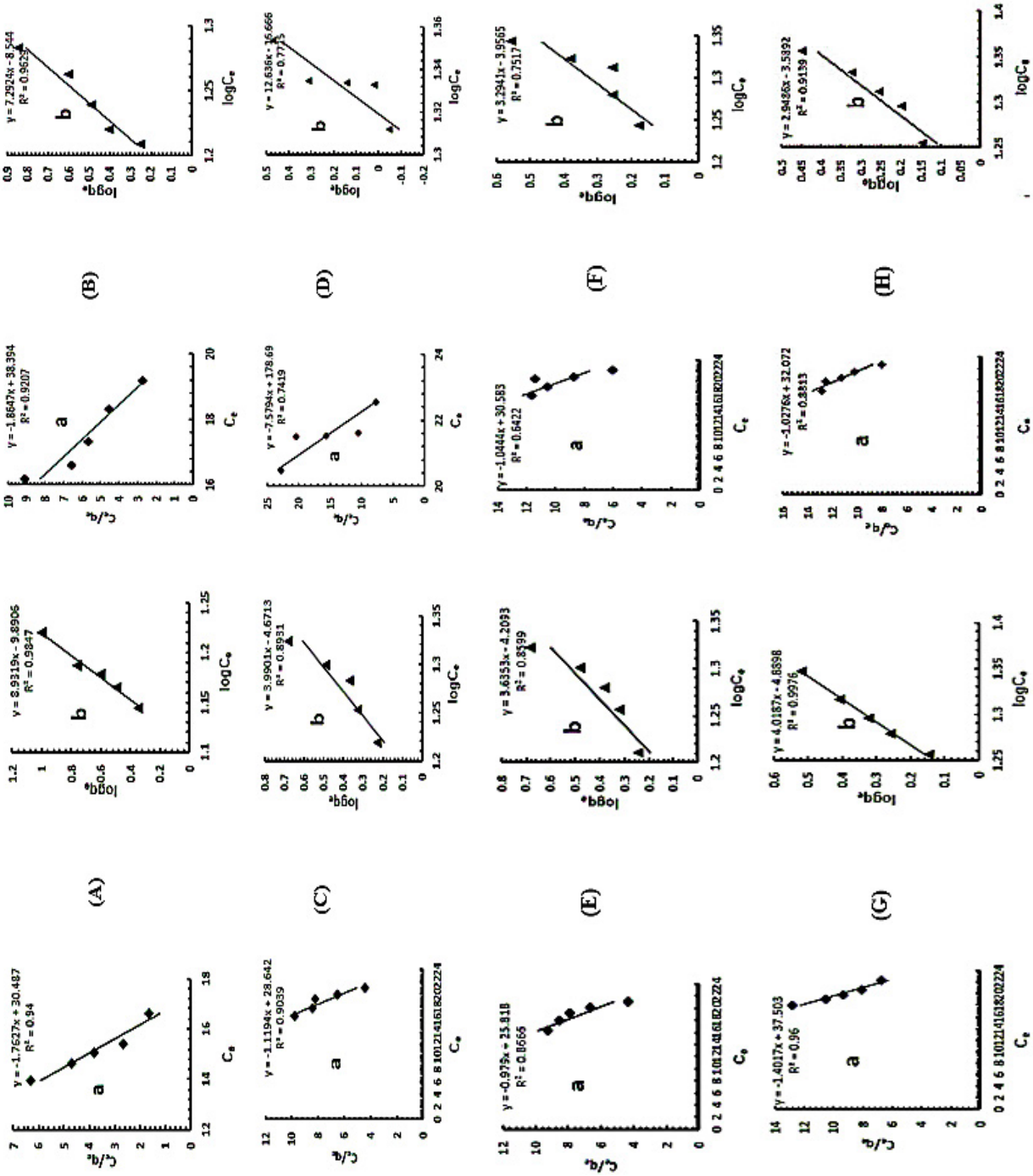

Fig. 20. Adsorption isotherm models with ACWS (a) Langmuir and (b) Freundlich. [A: 500°C & 20% H_3PO_4, B: 500°C & 40% H_3PO_4, C: 500°C & 60% H_3PO_4, D: 500°C & 80% H_3PO_4, E: 700°C & 20% H_3PO_4, F: 700°C & 40% H_3PO_4, G: 700°C & 60% H_3PO_4, H: 700°C & 80% H_3PO_4].

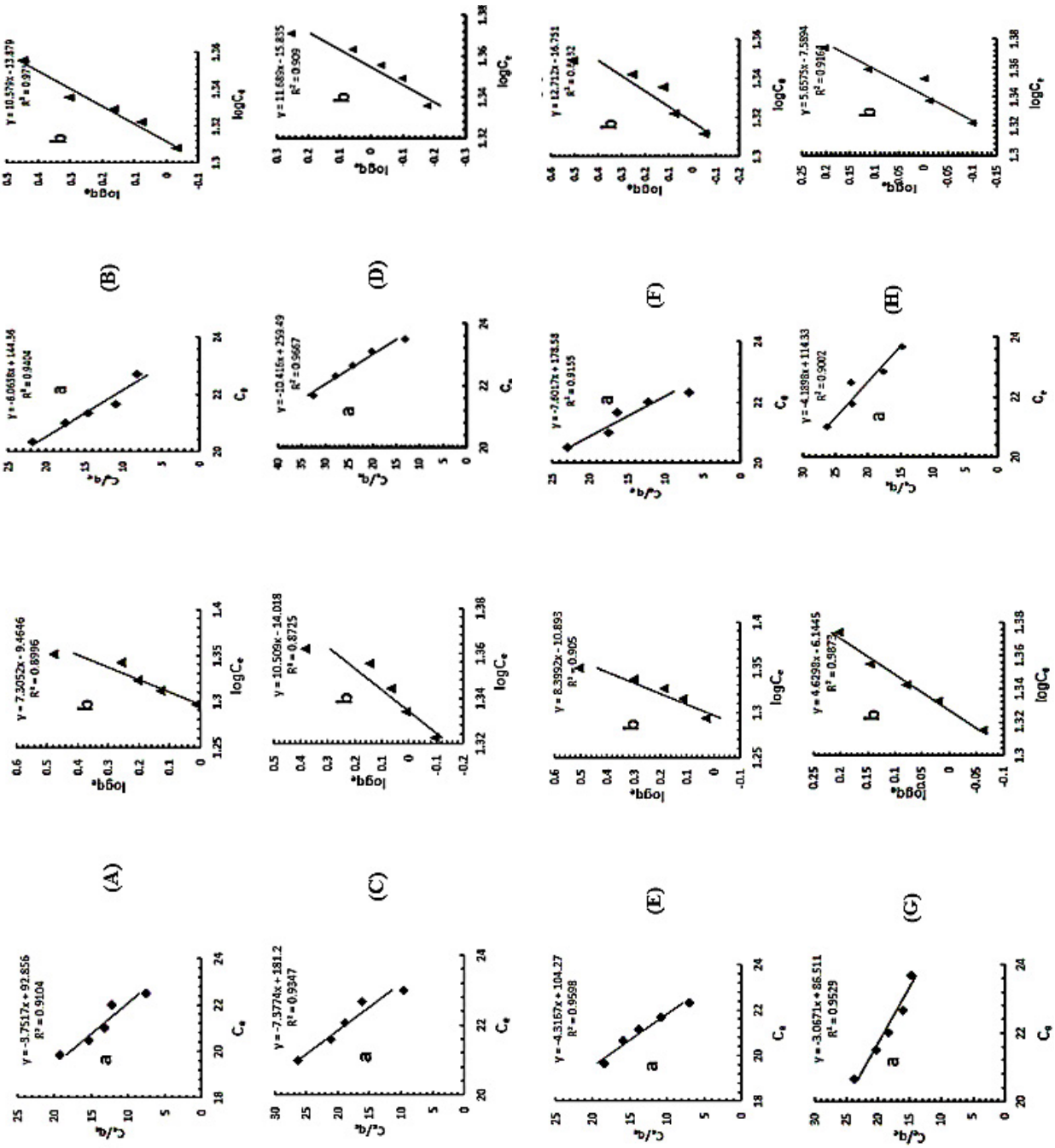

Fig. 21. Adsorption isotherm models with ACO (a) Langmuir and (b) Freundlich. [A: 500°C & 20% H_3PO_4, B: 500°C & 40% H_3PO_4, C: 500°C & 60% H_3PO_4, D: 500°C & 80% H_3PO_4, E: 700°C & 20% H_3PO_4, F: 700°C & 40% H_3PO_4, G: 700°C & 60% H_3PO_4, H: 700°C & 80% H_3PO_4].

and multilayer adsorption takes place in the system carbon-ion. Also, the obtained correlation coefficients (R^2) showed that the best isotherm model for adsorption of cadmium by ACWS and ACO with 20% phosphoric acid at 500°C were both Langmuir and Freundlich models. In general, among activation temperatures, 500°C is most appropriate for Langmuir and Freundlich models. The reason is that at this temperature activated carbon has a lignin structure which could avoid the pore blocking favoring the multi-layer sorption. Another parameter is n (Freundlich constant) and indicates the degree of surface heterogeneity in terms of adsorption sites, the value of which must be between 0 and 1 to indicate the desirability of the reaction. The closer n to each other, indicates the homogeneity of the adsorption sites and the small variety of surface adsorption sites. Conversely, when n tends to zero, the heterogeneity of adsorption sites increases, indicating that there is a wide range of adsorption sites. The K_F constant of the Freundlich equation indicates the relative adsorption capacity. The results showed the highest adsorption capacity of ACWS with 80% phosphoric acid at 500°C and 700°C and the highest adsorption capacity was found for ACO with 20% phosphoric acid at 500°C and activated carbon with 40% phosphoric acid at 700°C.

3.6. Kinetics study

Adsorption capacities of ACWS and ACO was tested as a function of time. All the adsorption rate constants and linear regression correlation coefficients are presented in Table 3. The results showed that for all adsorbents the adsorption–desorption equilibrium for cadmium was reached within 100 min. Fast adsorption of cadmium was observed in the first 80 min of contact time due to the maximum availability of unoccupied active sites on the adsorbents. Pseudo-first-order and pseudo-second-order models were applied to describe the kinetic isotherm. Pseudo-second-order model was the best fit for ACWS and pseudo-first-order model fitted to ACO. To verify the goodness of pseudo-first-order and pseudo-second-order models, in addition to the evaluation of R^2, it is necessary also to make a comparison between the q_e calculated by the models and the q_e experimentally measured. The pseudo-second-order model showed high R^2 values, but q_e calculated are quite different from the measured values, thus kinetics cannot be explained using the pseudo-second-order equation. A plausible explanation for the differences observed in adsorption velocities between the two particle sizes may relate to the structural differences.

4. Conclusion

Activated carbon, as green adsorbents, were prepared from walnut skin and ox tongue leftover for the sorption of cadmium from aqueous solutions by changing some parameters. The adsorption of cadmium was strongly depended on its initial concentration, contact time, pH, and the amount of adsorbent. 150 mg activated carbon made from ACWS and ACO removed 90.66% and 89.33% of cadmium content from 100 mL of 25 mg L^{-1} concentrated

Table 2
Langmuir and Freundlich isotherms parameters for cadmium adsorption on the ACWS and ACO

Adsorption isotherms			Freundlich						Langmuir					
			K_F (mg g^{-1})(L mg^{-1})$^{-1/n}$		n		R^2		Q (mg g^{-1})		b (L mg^{-1})		R_L		R^2	
T (°C)	H_3PO_4		ACWS	ACO	ACWS	ACO	ACWS	ACO	ACWS	ACO	ACWS	ACO	ACWS	ACO	ACWS	ACO
500	20%		1.28 ± 0.021	3.43 ± 0.52	0.11 ± 0.011	0.13 ± 0.021	0.98	0.85	0.56 ± 0.01	0.26 ± 0.002	0.05	0.04	0.4	0.4	0.94	0.91
500	40%		0.007 ± 0.001	1.32 ± 0.065	0.1 ± 0.013	0.09 ± 0.033	0.96	0.97	0.53 ± 0.005	0.16 ± 0.001	0.04	0.04	0.4	0.4	0.92	0.94
500	60%		0.002 ± 0.0008	0.5 ± 0.01	0.25 ± 0.022	0.09 ± 0.012	0.89	0.87	0.89 ± 0.002	0.13 ± 0.008	0.03	0.04	0.5	0.4	0.90	0.93
500	80%		2.15 ± 0.0013	1.4 ± 0.56	0.07 ± 0.031	0.08 ± 0.017	0.77	0.90	0.13 ± 0.003	0.09 ± 0.0008	0.04	0.04	0.48	0.4	0.74	0.96
700	20%		0.006 ± 0.0001	1.27 ± 0.091	0.27 ± 0.021	0.11 ± 0.015	0.85	0.90	1.02 ± 0.01	0.23 ± 0.011	0.03	0.04	0.51	0.4	0.86	0.95
700	40%		0.001 ± 0.001	1.77 ± 0.079	0.3 ± 0.033	0.07 ± 0.022	0.75	0.84	0.95 ± 0.019	0.13 ± 0.0014	0.03	0.04	0.53	0.4	0.64	0.91
700	60%		0.001 ± 0.0014	2.01 ± 0.081	0.24 ± 0.012	0.21 ± 0.022	0.99	0.98	0.71 ± 0.05	0.32 ± 0.091	0.03	0.03	0.51	0.53	0.96	0.95
700	80%		0.002 ± 0.0016	2.57 ± 0.568	0.3 ± 0.017	0.17 ± 0.031	0.91	0.91	0.97 ± 0.098	0.23 ± 0.05	0.03	0.03	0.55	0.52	0.88	0.90

Table 3
Kinetic parameters pertaining to the adsorption of cadmium onto ACWS and ACO

Kinetic		Pseudo-second-order						Pseudo-first-order					
		q_e (mg g^{-1})		k_2 (g mg^{-1} min^{-1})		R^2		q_e (mg g^{-1})		k_1 (min^{-1})		R^2	
T (°C)	H_3PO_4	ACWS	ACO	ACWS	ACO	ACWS	ACO	ACWS	ACO	ACWS	ACO	ACWS	ACO
500	20%	2.82	4.18	0.019	0.004	0.958	0.807	0.489	0.442	0.002	0.006	0.89	0.864
500	40%	2.17	7.21	0.032	0.001	0.993	0.275	0.507	0.413	0.003	0.005	0.88	0.843
500	60%	1.95	2.83	0.039	0.005	0.994	0.604	0.496	0.428	0.003	0.002	0.96	0.812
500	80%	1.51	1.88	0.070	0.016	0.996	0.521	0.489	0.367	0.002	0.003	0.89	0.837
700	20%	4.42	3.56	0.040	0.005	0.989	0.691	1.71	0.429	0.005	0.006	0.86	0.818
700	40%	4.46	3.12	0.028	0.006	0.996	0.937	1.04	0.445	0.011	0.004	0.97	0.853
700	60%	4.24	3.11	0.024	0.004	0.999	0.539	0.80	0.423	0.019	0.003	0.87	0.939
700	80%	4.11	250	0.015	3.059	0.933	7E-07	0.75	0.385	0.006	0.003	0.76	0.907

solution at 100 min and pH = 10, respectively. Also, the percentage of cadmium removal by inactivated charcoal of walnut skin and ox tongue leftover in optimal removal conditions at two temperatures of 500°C and 700°C was investigated, which was removed for walnut shell charcoal 60% and 55%, respectively and for charcoal obtained from ox tongue leftover 50% and 37%, respectively. The results illustrated that walnut shell is a more applicable material than ox tongue leftover for synthesis high quality activated carbon through chemical activation with different H_3PO_4 proportions. The results illustrated that walnut shell is a more applicable material than ox tongue leftover for synthesis high quality activated carbon through chemical activation with different H_3PO_4 proportions. Equilibrium studies indicated that the cadmium removal process on ACWS and ACO fitted to Langmuir and Freundlich isotherm models that this show the homogeneous and heterogeneous adsorption takes place in the system carbon-ion. Pseudo-second-order model was the best fit for ACWS and pseudo-first-order model for ACO. Functional groups such as carbonyl, hydroxide groups on the adsorbent surface were detected by using FT-IR analysis. FE-SEM images showed that ACO comprises closed pores with layer sheet structure and ACWS has open pores with regular sheet structure. According to these results, ACWS produced in this work are low-cost sorbents for removing cadmium from aqueous solutions.

Funding

This study has been performed with the financial support from the Larestan University of Medical Sciences, Larestan, Iran, Project No. 1399-58, and ethical code No. IRLARUMS. REC.1400.009.

Conflict of interests

The authors declare that there is no conflict of interests regarding the publication of this paper.

Data availability

All necessary data are present within the manuscript.

References

[1] M. Sharifirad, F. Kohyar, S.H. Rahmanpour, M. Vahidifar, Preparation of activated carbon from *Phragmites australis*: equilibrium and electrochemical behaviour study, Res. J. Recent Sci., 1 (2012) 10–16.
[2] G.P. Kumar, S.K. Yadav, P.R. Thawale, S.K. Singh, A.A. Juwarkar, Growth of *Jatropha curcas* on heavy metal contaminated soil amended with industrial wastes and *Azotobacter* – a greenhouse study, Bioresour. Technol., 99 (2008) 2078–2082.
[3] I. Anastopoulos, I. Massas, C. Ehaliotis, Use of residues and by-products of the olive-oil production chain for the removal of pollutants from environmental media: a review of batch biosorption approaches, J. Environ. Sci. Health. Part A Toxic/Hazard. Subst. Environ. Eng., 50 (2015) 677–718.
[4] S.E. Manahan, Environmental Chemistry, 8th ed., CRC Press LLC, New York, p. 765.
[5] M. Hua, S. Zhang, B. Pan, W. Zhang, L. Lv, Q. Zhang, Heavy metal removal from water/wastewater by nanosized metal oxides: a review, J. Hazard. Mater., 211 (2012) 317–331.
[6] E. Alvarez-Ayuso, A. García Sánchez, Removal of cadmium from aqueous solutions by palygorskite, J. Hazard. Mater., 147 (2007) 594–600.
[7] W.W. Eckenfelder, Industrial Water Pollution Control, 2nd ed., McGraw Hill, New York, 1989.
[8] S.S. Ahluwalia, D. Goyal, Microbial and plant derived biomass for removal of heavy metals from wastewater, Bioresour. Technol., 98 (2007) 2243–2257.
[9] J.T. Nwabanne, P.K. Igbokwe, Preparation of activated carbon from Nipa palm nut: influence of preparation conditions, Res. J. Recent Sci., 1 (2011) 53–58.
[10] I. Khazaei, M. Aliabadi, H.T. Hamed Mosavian, Use of agricultural waste for removal of Cr(VI) from aqueous solution, Iran. J. Chem. Chem. Eng., 8 (2011) 11–23.
[11] O.A. Ekpete, M. Horsfall, Preparation and characterization of activated carbon derived from fluted pumpkin stem waste (*Telfairia occidentalis Hook F*), Res. J. Chem. Sci., 1 (2011) 10–17.
[12] J.F. González, S. Román, C.M. González-García, J.M. Valente Nabais, A. Luis Ortiz, Porosity development in activated carbons prepared from walnut shells by carbon dioxide or steam activation, Ind. Eng. Chem. Res., 48 (2009) 7474–7481.
[13] M. Luo, H. Lin, B. Li, Y. Dong, Y. He, L. Wang, A novel modification of lignin on corncob-based biochar to enhance removal of cadmium from water, Bioresour. Technol., 259 (2018) 312–318.
[14] H. Li, X. Dong, E.B. da Silva, L.M. de Oliveira, Y. Chen, L.Q. Ma, Mechanisms of metal sorption by biochars: biochar characteristics and modifications, Chemosphere, 178 (2017) 466–478
[15] L. Trakal, V. Veselská, I. Šafařík, M. Vítková, S. Číhalová, M. Komárek, Lead and cadmium sorption mechanisms on

magnetically modified biochars, Bioresour. Technol., 203 (2016) 318–324.
[16] S.M. Anisuzzaman, C.G. Joseph, W.M. Ashri Bin Wan Daud, D. Krishnaiah, H.S. Yee, Preparation and characterization of activated carbon from *Typha orientalis* leaves, Int. J. Ind. Chem., 6 (2015) 9–21.
[17] W. Gao, M. Majumder, L.B. Alemany, T.N. Narayanan, M.A. Ibarra, B.K. Pradhan, P.M. Ajayan, Engineered graphite oxide materials for application in water purification, ACS Appl. Mater. Interfaces, 3 (2011) 1821–1826.
[18] Z. Li, Y. Kong, Y. Ge, Synthesis of porous lignin xanthate resin for Pb^{2+} removal from aqueous solution. Chem. Eng. J., 270 (2015) 229–234.
[19] V.B.H. Dang, H.D. Doan, T. Dang-Vu, A. Lohi, Equilibrium and kinetics of biosorption of cadmium(II) and copper(II) ions by wheat straw, Bioresour. Technol., 100 (2009) 211–219.
[20] S. Ul Mehdi, K, Aravamudan, Adsorption of cadmium ions on silica coated metal organic framework, Mater. Today:. Proc., (2022), doi: 10.1016/j.matpr.2021.12.304.
[21] E.-H. Ablouh, Z. Kassab, F.-z. Semlali Aouragh Hassani, M. El Achaby, H. Sehaqui, Phosphorylated cellulose paper as highly efficient adsorbent for cadmium heavy metal ion removal in aqueous solutions, RSC Adv., 12 (2022) 1084–1094.
[22] B. Kayranli, Cadmium removal mechanisms from aqueous solution by using recycled lignocelluloses, Alexandria Eng. J., 61 (2022) 443–457.
[23] A.A. Hezam Saeed, N.Y. Harun, M.M. Nasef, A. Al-Fakih, A.A.S. Ghaleb, H.K. Afolabi, Removal of cadmium from aqueous solution by optimized rice husk biochar using response surface methodology, Ain Shams Eng. J., 13 (2021) 101516, doi: 10.1016/j.asej.2021.06.002.
[24] T. Bandara, J. Xu, I.D. Potter, A. Franks, J.B.A.J. Chathurika, C. Tang, Mechanisms for the removal of Cd(II) and Cu(II) from aqueous solution and mine water by biochars derived from agricultural wastes, Chemosphere, 254 (2020) 126745, doi: 10.1016/j.chemosphere.2020.126745.
[25] D. Teng, B. Zhang, G. Xu, B. Wang, K. Mao, J. Wang, J. Sun, X. Feng, Z. Yang, H. Zhang, Efficient removal of Cd(II) from aqueous solution by pinecone biochar: sorption performance and governing mechanisms, Environ. Pollut., 265 (2020) 115001, doi: 10.1016/j.envpol.2020.115001.
[26] Z. Li, Y. Gong, D. Zhao, Z. Dang, Z. Lin, Enhanced removal of zinc and cadmium from water using carboxymethyl cellulose-bridged chlorapatite nanoparticles, Chemosphere, 263 (2021) 128038, doi: 10.1016/j.chemosphere.2020.128038.
[27] Y. Chen, H. Wang, W. Zhao, S. Huang, Four different kinds of peels as adsorbents for the removal of Cd(II) from aqueous solution: kinetics, isotherm and mechanism, J. Taiwan Inst. Chem. Eng., 88 (2018) 146–151.
[28] E. Jafarigol, R.A. Ghotli, A. Hajipour, H. Pahlevani, M.B. Salehi, Tough dual-network GAMAAX hydrogel for the efficient removal of cadmium and nickle ions in wastewater treatment applications, J. Ind. Eng. Chem., 94 (2021) 352–360.
[29] F.S. Higashikawa, R. Feola Conz, M. Colzato, C.E.P. Cerri, L.R. Ferracciú Alleoni, Effects of feedstock type and slow pyrolysis temperature in the production of biochars on the removal of cadmium and nickel from water, J. Cleaner Prod., 137 (2016) 965–972.
[30] Y. Li, M. Zhou, G.I.N. Waterhouse, J. Sun, W. Shi, S. Ai, Efficient removal of cadmium ions from water by adsorption on a magnetic carbon aerogel, Environ. Sci. Pollut. Res., 28 (2021) 5149–5157.